Physics Letters B 761 (2016) 344–349

Contents lists available at ScienceDirect

Physics Letters B

www.elsevier.com/locate/physletb

Investigating the jet activity accompanying the production at the LHC of a massive scalar particle decaying into photons

Benjamin Fuks [a,b], Dong Woo Kang [c,d], Seong Chan Park [d,e,*], Min-Seok Seo [f]

[a] Sorbonne Universités, UPMC Univ. Paris 06, UMR 7589, LPTHE, F-75005 Paris, France
[b] CNRS, UMR 7589, LPTHE, F-75005 Paris, France
[c] Department of Physics, Sungkyunkwan University, Suwon 440-746, Republic of Korea
[d] Dept. of Physics & IPAP, Yonsei University, Seoul 03722, Republic of Korea
[e] Korea Institute for Advanced Study (KIAS), Seoul 02455, Republic of Korea
[f] Center for Theoretical Physics of the Universe, Institute for Basic Science, 34051 Daejeon, Republic of Korea

ARTICLE INFO

Article history:
Received 30 July 2016
Received in revised form 24 August 2016
Accepted 26 August 2016
Available online 29 August 2016
Editor: J. Hisano

ABSTRACT

We study the jet activity that accompanies the production by gluon fusion of a new physics scalar particle decaying into photons at the LHC. In the considered scenarios, both the production and decay mechanisms are governed by loop-induced interactions involving a heavy colored state. We show that the presence of large new physics contributions to the inclusive diphoton invariant-mass spectrum always implies a significant production rate of non-standard diphoton events containing extra hard jets. We investigate the existence of possible handles that could provide a way to obtain information on the underlying physics behind the scalar resonance, and this in a wide mass window.

1. Introduction

The resonant production of a highly massive diphoton system consists of a prediction of many theories beyond the Standard Model, in particular in the case where the Higgs sector is non-minimal. Scrutinizing LHC proton–proton collisions giving rise to events featuring two hard photons plays thus a key role in the LHC experimental program, in particular as the diphoton channel is experimentally clean and associated with a small Standard Model background. The related Run I ATLAS and CMS analyses have hence been cornerstones for the Higgs boson discovery in 2012 [1,2], and the Run II has a great potential to observe a new massive particle decaying into two photons for masses ranging up to a few TeV [3–6]. More precisely, such a new particle should appear as a resonant bump in the diphoton invariant-mass spectrum. Previous hints at the 2σ-level for such a diphoton resonance have spurred an intense theoretical activity over the last few months, and different attempts have been performed in order to characterize the excess both from the top-down and bottom-up approaches. In the meantime, updated LHC results have been reported and a new physics signal now turns out to be statistically disfavored [7,8]. In this work, we motivate the study of less inclusive channels in order to verify the compatibility of the properties of any new state that would be decaying into a diphoton system with respect to QCD radiation.

As the Landau–Yang theorem [9,10] forbids the on-shell coupling of a massive vector boson to a photon pair and the off-shell case does not give rise to any resonant behavior, diphoton resonance searches are usually interpreted as limits on the existence of a scalar (with a spin $s = 0$) or a tensor (with a spin $s = 2$) state. In this paper, we focus on new physics setups featuring a massive scalar particle that we denote by R and refer to Ref. [11] for information on the spin-two case. In order for this particle to be produced with a sufficiently large rate to be observed in the diphoton mode, we assume that the couplings of the R particle to the Standard Model gluons and photons are issued from interactions with a new colored and electrically charged particle. We investigate two simplified models where this colored particle is either a heavy quark Q or a heavy scalar quark $\tilde{q}$. Both scenarios yield the loop-induced production of the R state via the gluon-fusion mechanism $gg \to R$, as depicted in Fig. 1 for the heavy quark case, and the R-decay mode into a photon pair $R \to \gamma\gamma$.

As shown in Fig. 2 where we present the leading-order Feynman diagrams corresponding to the production of the scalar particle R with an additional gluon via a loop containing the heavy quark state Q, the interactions under consideration also induce the associated production of the R particle with additional jets. We re-

* Corresponding author.
E-mail address: sc.park@yonsei.ac.kr (S.C. Park).

http://dx.doi.org/10.1016/j.physletb.2016.08.056

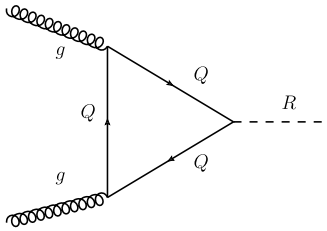

Fig. 1. Feynman diagram representing the loop-induced production of a scalar R-particle via gluon fusion when a heavy quark Q runs into the loop.

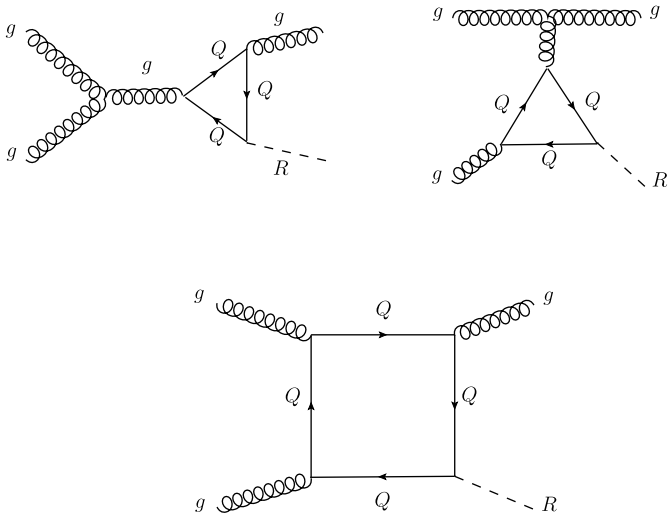

Fig. 2. Feynman diagrams representing the loop-induced production of a scalar particle R in association with a hard jet, via gluon fusion and when a heavy quark Q runs into the loop. The two diagrams in the first row are triangle ($\triangle$) diagrams and the one in the second row is a box ($\square$) diagram.

strict our study to a configuration featuring one extra jet with a transverse-momentum of at least 50–100 GeV, as the magnitude of the cross section related to the production of the R state with two or more such hard jets is estimated to be too small to yield any statistically meaningful deviation within the context of the current amount of recorded LHC data. There are two categories of diagrams contributing to the $gg \to Rg$ process respectively containing a triangular loop (the so-called *triangle* diagrams $\triangle$ presented in the upper panel of the figure) and a rectangular loop (the so-called *box* diagram $\square$ of the lower panel of the figure), the triangle diagrams sharing the same vertex structure as for single R production. Since this process is loop-induced, the corresponding scattering amplitude is ultraviolet finite. It nonetheless exhibits infrared divergences related to the extra gluon that could be soft, collinear or both. The phase space integration can however be safely performed thanks to the requirement of this gluon being hard, which prevents from entering the infrared sensitive phase space regions. In the following, we investigate how measurements of the properties of the jets produced in association with a scalar diphoton resonance can provide new handles to probe the underlying physics. Our study complements recent works in which the jet multiplicity spectrum associated with the production of the R particle with a mass fixed to 750 GeV has been probed to get information on the production mechanism from which the diphoton signal originates [11–13] or in which effective field theory limits are studied [14].

While the latter work mostly focuses on non-renormalizable dimension-five operators describing the new physics, we in contrast consider a theoretical framework containing only renormalizable four-dimensional operators. By performing exact one-loop calculations, we probe both the structure of the loop-diagrams giving rise to a diphoton signal with and without extra hard jets and the structure of the couplings of the R particle to the Standard Model.

In the next section (Section 2), we describe the theoretical setup employed for our analysis and then present our phenomenological results in Section 3. We conclude and summarize our findings in Section 4.

2. Theoretical framework

In our study, we assume the existence of a real scalar field R with a mass m_R whose interactions with the Standard Model are mediated via the exchange of a heavy quark Q of mass m_Q. Vector-like quarks are important in many extensions of the Standard Model (*e.g.* in theories with extra dimensions [15,16] or composite-Higgs models with partial compositeness [17]) and are generally considered as lying in the fundamental representation of the QCD gauge group $\mathrm{SU}(3)_c$. Although they can possibly lie in many different representations of the electroweak symmetry group $\mathrm{SU}(2)_L \times \mathrm{U}(1)_Y$, we focus on a minimal setup where the Q quark is a weak isospin singlet with an hypercharge quantum number set to 2/3. In addition, we neglect any mixing with the Standard Model up-type quark sector, so that we rely on the effective new physics Lagrangian

$$\mathcal{L}^{(1)}_{\rm NP} = i\bar{Q}\not{\partial}Q - m_Q\,\bar{Q}\,Q + \frac{1}{2}\partial_\mu R\partial^\mu R - \frac{1}{2}m_R^2R^2 + \hat{\kappa}_Q\,R\,\bar{Q}\,Q\ , \tag{1}$$

that is supplemented to the Standard Model Lagrangian $\mathcal{L}_{\rm SM}$. The interaction strength between the heavy quark and R is denoted by $\hat{\kappa}_Q$, and the gauge covariant derivative is given by

$$D_\mu Q = \partial_\mu Q - ig_sT_aG^a_\mu Q - i\frac{2}{3}eA_\mu Q\ , \tag{2}$$

with g_s and e denoting the strong and electromagnetic coupling constants, G_μ and A_μ the gluon and photon fields and T_a the fundamental representation matrices of $SU(3)$. Since the extra quark Q does not mix with the Standard Model quark sector, our new physics model evades by construction all existing searches for vector-like quarks at the LHC [18–22]. As a result, our simple parameterization also embeds models in which there are more than one state connecting the R scalar to the Standard Model. This can be accounted for by a stronger $\hat{\kappa}_Q$ coupling.

Alternatively, one may consider that the mediation of the new physics interactions of the R particle with the Standard Model proceeds via the exchange of a scalar quark $\tilde{q}$ of mass $m_{\tilde{q}}$. For the sake of minimality and simplicity, the squark $\tilde{q}$ is considered as a weak isospin singlet and lies in the fundamental representation of the $SU(3)_c$ group. The new physics sector is then described by the Lagrangian

$$\mathcal{L}^{(2)}_{\rm NP} = D_\mu\tilde{q}^\dagger D^\mu\tilde{q} - m^2_{\tilde{q}}\tilde{q}^\dagger\tilde{q} + \frac{1}{2}\partial_\mu R\partial^\mu R - \frac{1}{2}m_R^2R^2 + \hat{\kappa}_{\tilde{q}}R\,\tilde{q}^\dagger\tilde{q}\ . \tag{3}$$

In the next section, we will investigate the effects related to the nature of the particle connecting the new physics to the Standard Model sectors, and make predictions by using either the Lagrangian $\mathcal{L}^{(1)}_{\rm NP}$ or the Lagrangian $\mathcal{L}^{(2)}_{\rm NP}$. As for the vector-like quark case, the squark $\tilde{q}$ does not singly couple to the Standard Model so that our new physics modeling cannot be probed by typical squark searches at the LHC.

In order to calculate (loop-induced) differential and total cross sections related to processes involving an R scalar in the final state, we make use of the MadGraph5_aMC@NLO platform [23]

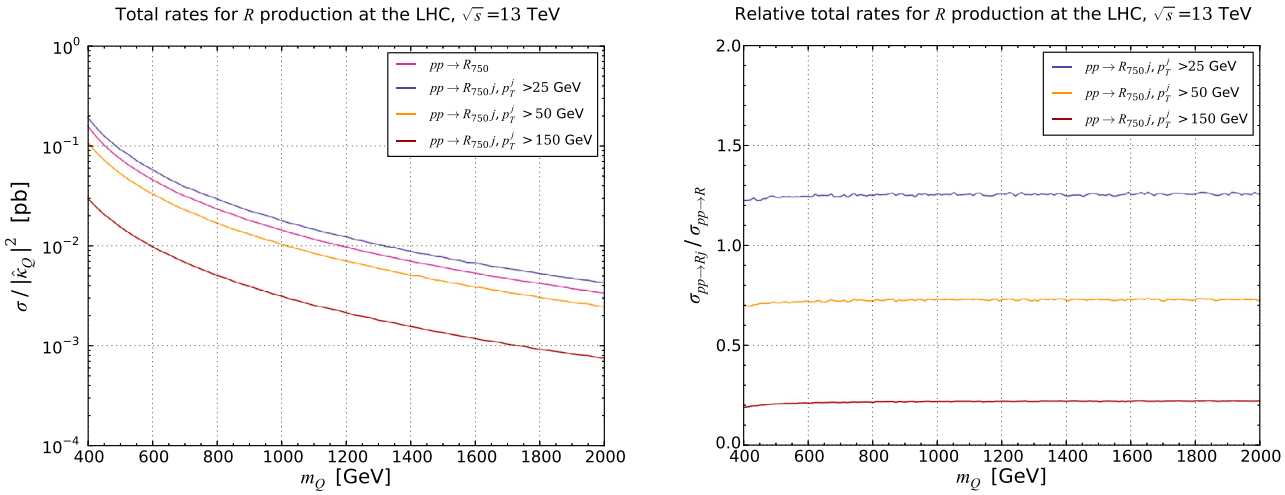

Fig. 3. Total production cross sections for the production of a 750 GeV scalar resonance, possibly in association with a jet whose transverse momentum is imposed to be above a specific threshold. In the right panel of the figure, we present the production rates relatively to the $pp \to R$ total production cross section. All results are presented as function of the mass of the vector-like quark Q running into the loop m_Q. (For interpretation of the references to color in this figure legend, the reader is referred to the web version of this article.)

whose loop-module [24] has been recently extended to deal with loop-induced processes [25]. This relies on the numerical evaluation of loop integrals in four dimensions, which necessitates the calculation of rational terms associated with the ϵ-dimensional components of the loop-integrals that should be normally evaluated in $D = 4 - 2\epsilon$ dimensions. These rational terms can be split into two ensembles, the first one being connected to the loop-integral denominators (R_1) and the second one to the loop-integral numerators (R_2). While the R_1 terms are universal, the R_2 terms are model-dependent and process-dependent. They can however be cast as a finite number of counterterm Feynman rules derived from the bare Lagrangian [26]. Starting from the two $\mathcal{L}^{(i)}_{\rm NP}$ Lagrangians, we translate, by a joint use of the FeynRules [27] and NLOCT [28] packages, the model information into a UFO library [29] that contains all relevant R_2 counterterms and that is ready to be used in MadGraph5_aMC@NLO.

3. Phenomenological results

As a first benchmark scenario, we focus on the possible characterization of the 750 GeV resonance whose hints have been recently observed by both the ATLAS and CMS collaborations [3,4]. To this aim, it is useful to study its production together with a possible additional hard jet.

In Fig. 3, we consider a model where the coupling of the R scalar with the Standard Model occurs via heavy Q-quark exchanges (the model described by the $\mathcal{L}^{(1)}_{\rm NP}$ Lagrangian of Eq. (1)), and we evaluate total cross sections for R production possibly in association with a jet whose transverse momentum p_T is constrained to be above some threshold p_T^j. In our calculations, the loop-induced hard matrix elements have been convoluted with the next-to-leading order set of NNPDF 3.0 parton distribution functions [30] accessed via the LHAPDF 6 library [31], and we have fixed both the factorization and renormalization scales to half the transverse mass of all final state particles. The results are presented with the $\hat{\kappa}_Q$ dependence of the cross sections factorized out, since the latter parameter can always be tuned so that the rate for $pp \to R$ accommodates any diphoton excess that would be observed, and as a function of the mass of the heavy quark Q that runs into the loops. Focusing, for the sake of the example, on a benchmark scenario in which $m_R = 750$ GeV and that corresponds to the Run II ATLAS and CMS past observations, vector-like quark masses ranging up to at most 2 TeV could accommodate a signal cross section of the order of 10–20 fb and simultaneously forbid the $\hat{\kappa}_Q$ value to be such that perturbation theory breaks down ($\hat{\kappa}_Q \lesssim 10$).

Comparing the $pp \to R$ to the $pp \to Rj$ predictions, we observe that any sign for a large beyond the Standard Model contribution to the diphoton production cross section $\sigma(pp \to R \to \gamma\gamma)$ is always accompanied with significant new physics effects in the production rate of diphoton events with extra hard jets. In our parameterization of Eq. (1), we have considered vector-like quarks lying in the fundamental representation of the $SU(3)$ group. However, the cross section ratios (right panel of Fig. 3) are independent of the color representation that could be chosen differently, resulting in larger rates. The effect of a different color representation choice for the heavy quark is related to the $SU(3)$ group theory factors of the different scattering amplitudes,

$$\mathcal{A}(g^a g^b \to R) \propto \mathrm{Tr}(T^a T^b) = \delta^{ab}/2, \tag{4}$$

$$\mathcal{A}_\triangle(g^a g^b \to R g^c) \propto \sum_d f^{abd}\mathrm{Tr}(T^d T^c) \propto \frac{1}{2} f^{abc}, \tag{5}$$

$$\mathcal{A}_\square(g^a g^b \to R g^c) \propto \mathrm{Tr}(T^a [T^b, T^c]) \propto \frac{1}{2} f^{abc}, \tag{6}$$

where a, b and c are the color indices carried by the initial-state and final-state gluons, and $\mathcal{A}_\triangle$ and $\mathcal{A}_\square$ are the one-loop amplitudes related to the $gg \to Rg$ process when considering either the triangle or the box diagrams respectively. The amplitudes are hence all independent of the specific color representation of the heavy quark.

Investigating the $pp \to Rj$ process, it turns out that the full amplitude exhibits a t-channel enhancement such that the contributions from the triangle diagrams dominate over the box diagram ones, especially when the mass of the quark Q is not too large. This 'triangle dominance' consequently implies that the ratio $\sigma(pp \to Rj)/\sigma(pp \to R)$ is insensitive to the quark mass m_Q in the mass window of interest, since the same triangle loop approximately factorizes from the two amplitudes $\mathcal{A}(gg \to R)$ and $\mathcal{A}(gg \to Rg) = \mathcal{A}_\triangle(gg \to Rg) + \mathcal{A}_\square(gg \to Rg)$. The dependence of the results on the vector-like quark mass m_Q therefore stems

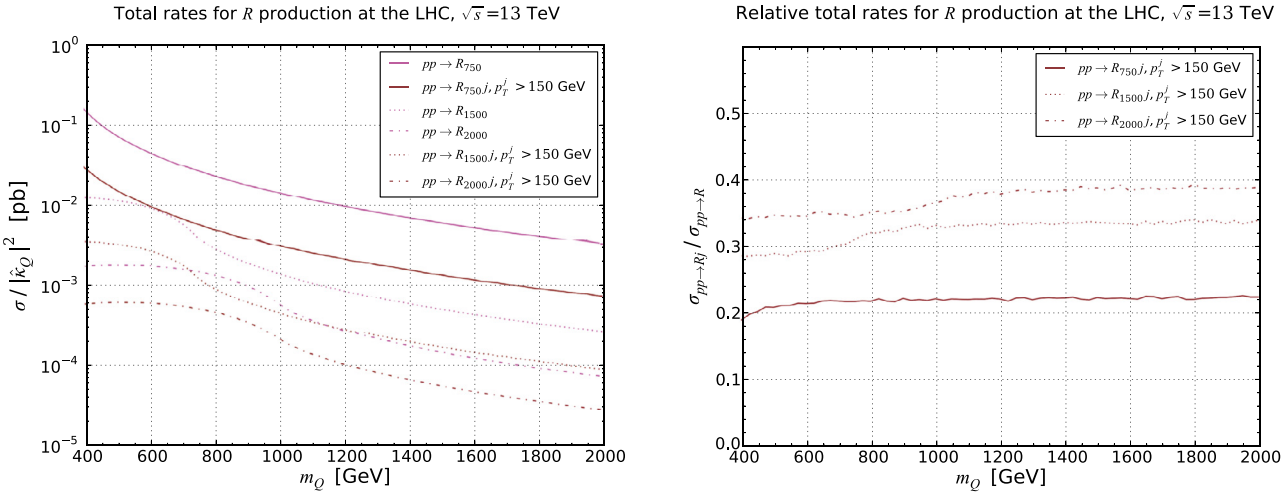

Fig. 4. Total production cross sections for the production of a massive scalar resonance, possibly in association with a jet whose transverse momentum is imposed to be above a specific threshold. In the right panel of the figure, we present the production rates relatively to the $pp \to R$ total production cross section. We focus on three scenarios for which $m_R = 750$ GeV, 1500 GeV and 2000 GeV respectively. (For interpretation of the references to color in this figure legend, the reader is referred to the web version of this article.)

from the form of the triangle-loop amplitude $\mathcal{A}_\triangle^{(1)}$ that is given, in the large m_Q limit, by

$$\mathcal{A}_\triangle^{(1)}(m_Q, m_R) \propto \frac{1}{m_Q} + \frac{7m_R^2}{120m_Q^3} + \frac{m_R^4}{168m_Q^5} + \mathcal{O}\left(\frac{m_R^6}{m_Q^7}\right). \tag{7}$$

In Fig. 4, we study the dependence of the previous results on the mass of the resonance m_R, and focus on two extra benchmark scenarios where m_R is fixed to 1500 GeV and 2000 GeV respectively. On the left panel of the figure, we show that the total rate is reduced when considering heavier R states, as could be expected from the corresponding phase space suppression and the dependence of $\mathcal{A}_\triangle^{(1)}$ on m_R. We can also observe the presence of threshold effects related to the imaginary part of the loop-amplitude when the vector-like quark mass is about half the R scalar mass. Such setups will nevertheless not be considered in the following, as in this case the scalar particle preferably decays back into a pair of vector-like quarks (that occurs at the tree level) and not into a photon pair (that is a loop-induced process). On the right panel of the figure, we present the dependence of the $\sigma(pp \to Rj)/\sigma(pp \to R)$ ratio in terms of the vector-like quark mass. We find that the cross section for producing the scalar state in association with a hard jet is relatively larger and larger for heavier and heavier R states. This property originates from two contributions, the renormalization scale choice (and the associated α_s value) that depends on m_R as well as the m_R functional form of the triangle loop-amplitude (see Eq. (7)). The α_s dependence is however reduced when comparing the two large R-mass values.

Similar conclusions could be observed for the new physics parameterization of Eq. (3) as the results of Eq. (4), Eq. (5) and Eq. (6) are general enough to hold regardless of the nature of the particle mediating the R coupling to the Standard Model.

The loop amplitude is however suppressed by one extra factor of the mass of the scalar quark running into the loop,

$$\mathcal{A}_\triangle^{(2)}(m_{\tilde{q}}, m_R) \propto \frac{1}{4m_{\tilde{q}}^2} + \frac{m_R^2}{30m_{\tilde{q}}^4} + \frac{3m_R^4}{560m_{\tilde{q}}^6} + \mathcal{O}\left(\frac{m_R^6}{m_{\tilde{q}}^8}\right), \tag{8}$$

so that it is not possible to simultaneously explain any potential excess of about 10–20 fb in the diphoton spectrum and maintain the perturbativity of the theory. Scenarios with extra squarks will therefore not be considered in the rest of this work.

In order to study the properties of a scalar diphoton resonance, it may be useful to investigate events where the new heavy particle recoils against a hard jet. For a proper description of such an event configuration, it is necessary to include at least one extra radiation at the level of the matrix element and match the fixed-order results to parton showers for a correct modeling of the remaining jet activity. We make use of the MadSpin [32] and MadWidth [33] programs to simulate the decay of the scalar R particle on the basis of the associated matrix element, after shrinking the $R\gamma\gamma$ loop-induced interaction to a point-like vertex. We then interface the partonic events obtained in this way to the parton showering and hadronization infrastructure implemented in the Pythia 8 package [34], and reconstruct all final state jets by means of the anti-k_T algorithm [35] with a radius parameter fixed to 0.4 as implemented in FastJet [36]. We finally analyze the generated events by means of the MadAnalysis 5 platform [37].

In Fig. 5, we study the properties of the diphoton system originating from the decay of the R particle (when produced in association with a hard jet) whose mass has been fixed to $m_R = 750$ GeV both in the case where the heavy quark mass is set to 500 GeV (solid blue curve) and when it is set to 1500 GeV (solid red line). Our results include a selection on the leading final-state jet, its transverse momentum p_T being imposed to be larger than 150 GeV and the absolute value of its pseudorapidity $|\eta|$ to be smaller than 2.5. On the upper panel of the figure, we present the transverse momentum distribution of the two final-state photons, and their angular distances in the transverse plane and in azimuth are shown in the lower panel of the figure. Except the normalization, the shapes of the spectra are very similar regardless of the vector-like quark mass choice, and this for all represented distributions. Although an inclusive diphoton signal is in general accompanied by a diphoton plus a hard jet signal, it is very unlikely that the photon properties could help on getting information on the vector-like quark state running into the loop. We additionally study two scenarios for which $m_Q = 1500$ GeV and m_R is respectively fixed to 1.5 TeV (green dotted line) and 2 TeV (purple dotted line). The conclusions are similar, with the difference in the shapes of the distributions being driven by the R state mass.

4. Conclusion

We have studied an extension of the Standard Model containing a singlet scalar particle R interacting with a new heavy col-

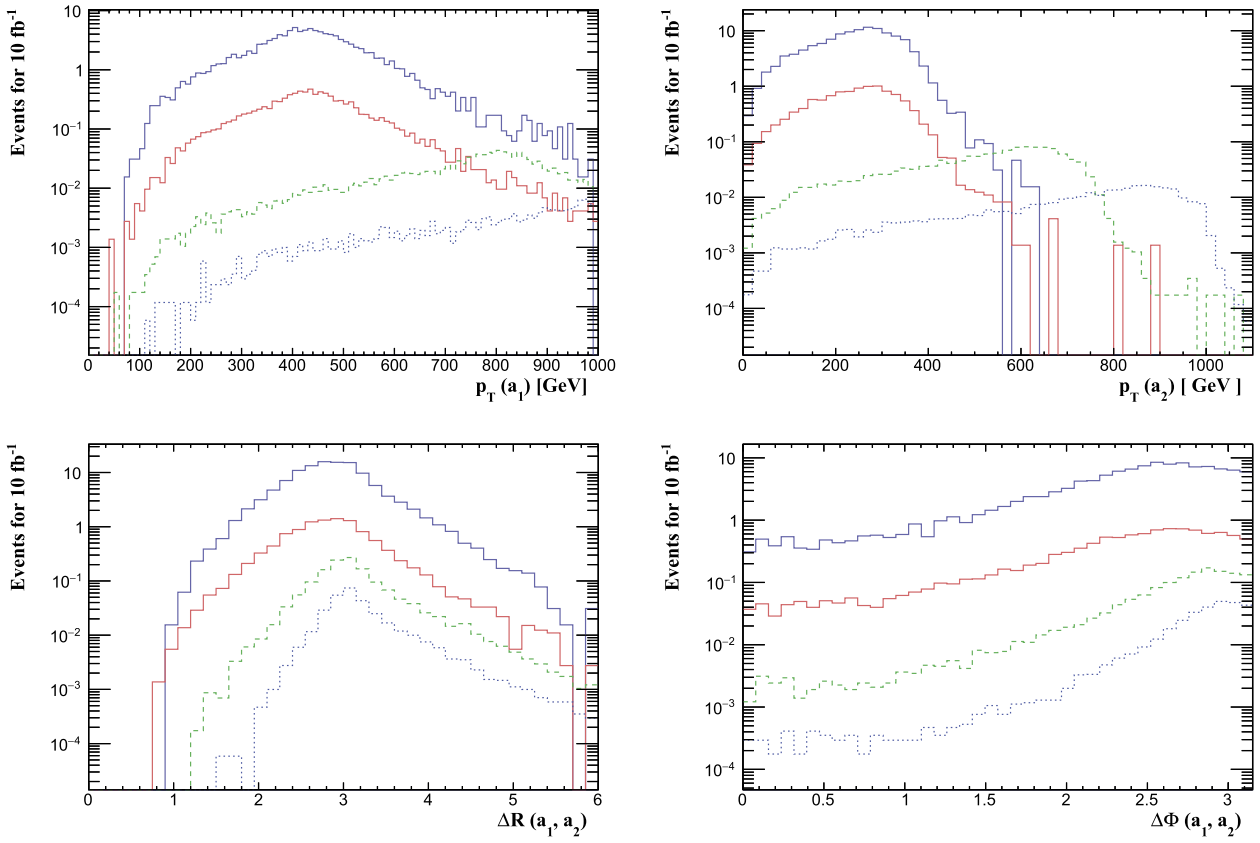

Fig. 5. Properties of the photon-pair originating from the decay of an R-particle produced in association with a hard jet. We present the transverse momentum spectrum of the leading and next-to-leading photons (top panel), their angular distance in the transverse plane (lower left panel) and their angular distance in azimuth (lower right panel). The vector-like quark mass is fixed either to 500 GeV (solid blue) or the 1500 GeV (solid red) for $m_R = 750$ GeV, and to 1500 GeV for scenarios in which $m_R = 1500$ GeV (green dotted) and 2000 GeV (purple dotted). The normalization assumes 10 fb^{-1} of 13 TeV LHC collisions. (For interpretation of the references to color in this figure legend, the reader is referred to the web version of this article.)

ored quark Q (with a spin $s = 1/2$) or squark $\tilde{q}$ (with a spin $s = 0$) through which the singlet scalar can be produced at the LHC by gluon fusion and decay into a diphoton system. We have pointed out that the observation of additional jet activity around an R-induced photon pair is important for checking the consistency of the underlying physics, as significant extra jet production is also predicted.

The rate for producing an additional hard jet at the LHC, evaluated relatively to the R single production cross section has been found to be around 20–40%, the exact value depending on the mass of the resonance particle m_R that we have varied in the 750–2000 GeV mass window. It is however less sensitive to the mass of the particle running into the loop amplitude, m_Q and $m_{\tilde{q}}$ for scenarios with a vector-like quark and scalar quark respectively. The properties of the primary and secondary photons issued from the R decay have also been investigated, and we have found that they do not seem to provide additional information on the colored particle running into the loop other than related to the overall normalization of the considered distributions, which is expected in the case of a scalar particle decay. We therefore strongly recommend to correlate the future inclusive analyses of highly massive diphoton systems at the LHC with less inclusive analyses imposing strong requirements on the underlying jet activity.

Acknowledgements

BF has been supported by the *Théorie LHC France* initiative of the CNRS (INP/IN2P3), SC by the National Research Foundation of Korea (NRF) grant funded by the Korean government (MSIP) (No. 2016R1A2B2016112) and MS by IBS (Project Code IBS-R018-D1).

References

[1] ATLAS collaboration, G. Aad, et al., Observation of a new particle in the search for the Standard Model Higgs boson with the ATLAS detector at the LHC, Phys. Lett. B 716 (2012) 1–29, arXiv:1207.7214.

[2] CMS collaboration, S. Chatrchyan, et al., Observation of a new boson at a mass of 125 GeV with the CMS experiment at the LHC, Phys. Lett. B 716 (2012) 30–61, arXiv:1207.7235.

[3] ATLAS collaboration, Search for resonances decaying to photon pairs in 3.2 fb^{-1} of pp collisions at $\sqrt{s} = 13$ TeV with the ATLAS detector, ATLAS-CONF-2015-081.

[4] CMS collaboration, Search for new physics in high mass diphoton events in proton–proton collisions at 13 TeV, CMS-PAS-EXO-15-004.

[5] ATLAS collaboration, Search for resonances in diphoton events with the ATLAS detector at $\sqrt{s} = 13$ TeV, ATLAS-CONF-2016-018.

[6] CMS collaboration, Search for new physics in high mass diphoton events in 3.3 fb^{-1} of proton–proton collisions at $\sqrt{s} = 13$ TeV and combined interpretation of searches at 8 TeV and 13 TeV, CMS-PAS-EXO-16-018.

[7] ATLAS collaboration, Search for scalar diphoton resonances with 15.4 fb^{-1} of data collected at $\sqrt{s} = 13$ TeV, in 2015 and 2016 with the ATLAS detector, ATLAS-CONF-2016-059.

[8] CMS collaboration, Search for resonant production of high mass photon pairs using 12.9 fb^{-1} of proton–proton collisions at $\sqrt{s} = 13$ TeV and combined interpretation of searches at 8 and 13 TeV, CMS-PAS-EXO-16-027.

[9] L.D. Landau, On the angular momentum of a system of two photons, Dokl. Akad. Nauk Ser. Fiz. 60 (1948) 207–209.

[10] C.-N. Yang, Selection rules for the dematerialization of a particle into two photons, Phys. Rev. 77 (1950) 242–245.

[11] J. Bernon, A. Goudelis, S. Kraml, K. Mawatari, D. Sengupta, Characterising the 750 GeV diphoton excess, J. High Energy Phys. 05 (2016) 128, arXiv:1603.03421.
[12] L.A. Harland-Lang, V.A. Khoze, M.G. Ryskin, M. Spannowsky, Jet activity as a probe of diphoton resonance production, arXiv:1606.04902.
[13] M.A. Ebert, S. Liebler, I. Moult, I.W. Stewart, F.J. Tackmann, K. Tackmann, et al., Exploiting jet binning to identify the initial state of high-mass resonances, arXiv:1605.06114.
[14] A. de la Puente, D. Stolarski, Breakdown of effective field theory for a gluon initiated resonance, arXiv:1607.04276.
[15] S.C. Park, J. Shu, Split universal extra dimensions and dark matter, Phys. Rev. D 79 (2009) 091702, arXiv:0901.0720.
[16] K. Kong, S.C. Park, T.G. Rizzo, A vector-like fourth generation with a discrete symmetry from Split-UED, J. High Energy Phys. 07 (2010) 059, arXiv:1004.4635.
[17] D.B. Kaplan, Flavor at SSC energies: a new mechanism for dynamically generated fermion masses, Nucl. Phys. B 365 (1991) 259–278.
[18] ATLAS collaboration, G. Aad, et al., Search for pair production of a new heavy quark that decays into a W boson and a light quark in pp collisions at $\sqrt{s} = 8$ TeV with the ATLAS detector, Phys. Rev. D 92 (2015), CERN-PH-EP-2015-212, arXiv:1509.04261.
[19] ATLAS collaboration, G. Aad, et al., Search for production of vector-like quark pairs and of four top quarks in the lepton-plus-jets final state in pp collisions at $\sqrt{s} = 8$ TeV with the ATLAS detector, J. High Energy Phys. 08 (2015), CERN-PH-EP-2015-095, arXiv:1505.04306.
[20] CMS collaboration, Search for single production of a vector like T quark decaying to a Higgs Boson and a leptonically decaying top quark, CMS-PAS-B2G-15-008.
[21] CMS collaboration, Search for top quark partners with charge 5/3 at $\sqrt{s} = 13$ TeV, CMS-PAS-B2G-15-006.
[22] ATLAS collaboration, Search for new physics using events with b-jets and a pair of same charge leptons in 3.2 fb^{-1} of pp collisions at $\sqrt{s} = 13$ TeV with the ATLAS detector, ATLAS-CONF-2016-032.
[23] J. Alwall, R. Frederix, S. Frixione, V. Hirschi, F. Maltoni, O. Mattelaer, et al., The automated computation of tree-level and next-to-leading order differential cross sections, and their matching to parton shower simulations, J. High Energy Phys. 07 (2014) 079, arXiv:1405.0301.
[24] V. Hirschi, R. Frederix, S. Frixione, M.V. Garzelli, F. Maltoni, R. Pittau, Automation of one-loop QCD corrections, J. High Energy Phys. 05 (2011) 044, arXiv:1103.0621.
[25] V. Hirschi, O. Mattelaer, Automated event generation for loop-induced processes, J. High Energy Phys. 10 (2015) 146, arXiv:1507.00020.
[26] G. Ossola, C.G. Papadopoulos, R. Pittau, On the rational terms of the one-loop amplitudes, J. High Energy Phys. 05 (2008) 004, arXiv:0802.1876.
[27] A. Alloul, N.D. Christensen, C. Degrande, C. Duhr, B. Fuks, FeynRules 2.0 — a complete toolbox for tree-level phenomenology, Comput. Phys. Commun. 185 (2014) 2250–2300, arXiv:1310.1921.
[28] C. Degrande, Automatic evaluation of UV and R2 terms for beyond the Standard Model Lagrangians: a proof-of-principle, Comput. Phys. Commun. 197 (2015) 239–262, arXiv:1406.3030.
[29] C. Degrande, C. Duhr, B. Fuks, D. Grellscheid, O. Mattelaer, T. Reiter, UFO — The Universal FeynRules Output, Comput. Phys. Commun. 183 (2012) 1201–1214, arXiv:1108.2040.
[30] NNPDF collaboration, R.D. Ball, et al., Parton distributions for the LHC Run II, J. High Energy Phys. 04 (2015) 040, arXiv:1410.8849.
[31] A. Buckley, J. Ferrando, S. Lloyd, K. Nordström, B. Page, M. Rüfenacht, et al., LHAPDF6: parton density access in the LHC precision era, Eur. Phys. J. C 75 (2015) 132, arXiv:1412.7420.
[32] P. Artoisenet, R. Frederix, O. Mattelaer, R. Rietkerk, Automatic spin-entangled decays of heavy resonances in Monte Carlo simulations, J. High Energy Phys. 03 (2013) 015, arXiv:1212.3460.
[33] J. Alwall, C. Duhr, B. Fuks, O. Mattelaer, D.G. Öztürk, C.-H. Shen, Computing decay rates for new physics theories with FeynRules and MadGraph 5_aMC@NLO, Comput. Phys. Commun. 197 (2015) 312–323, arXiv:1402.1178.
[34] T. Sjöstrand, S. Ask, J.R. Christiansen, R. Corke, N. Desai, P. Ilten, et al., An introduction to PYTHIA 8.2, Comput. Phys. Commun. 191 (2015) 159–177, arXiv:1410.3012.
[35] M. Cacciari, G.P. Salam, G. Soyez, The anti-k_t jet clustering algorithm, J. High Energy Phys. 04 (2008) 063, arXiv:0802.1189.
[36] M. Cacciari, G.P. Salam, G. Soyez, FastJet user manual, Eur. Phys. J. C 72 (2012) 1896, arXiv:1111.6097.
[37] E. Conte, B. Fuks, G. Serret, MadAnalysis 5, a user-friendly framework for collider phenomenology, Comput. Phys. Commun. 184 (2013) 222–256, arXiv:1206.1599.